

Identification of Shallow Trap Centers in InSe Single Crystals and Investigation of Their Distribution: A Thermally Stimulated Current Spectroscopy

M. Isik^{a,b,c}, N.M. Gasanly^{d,e}

^aDepartment of Biomedical Engineering, Faculty of Engineering and Architecture, İzmir Bakırçay University, 35665, İzmir, Türkiye

^bBiomedical Technologies Design Application and Research Center, İzmir Bakırçay University, 35665, İzmir, Türkiye

^cDepartment of Electrical and Electronics Engineering, Atılım University, 06836 Ankara, Türkiye

^dDepartment of Physics, Middle East Technical University, 06800 Ankara, Türkiye

^eVirtual International Scientific Research Centre, Baku State University, 1148 Baku, Azerbaijan

Abstract

Identification of trap centers in semiconductors takes great importance for improving the performance of electronic and optoelectronic devices. In the present study, we employed the thermally stimulated current (TSC) method within a temperature range of 10-280 K to explore trap centers in InSe crystal—a material with promising applications in next-generation devices. Our findings revealed the existence of two distinct hole trap centers within the InSe crystal lattice located at 0.06 and 0.14 eV. Through the leveraging the T_{stop} method, we offered trap distribution parameters of revealed centers. The results obtained from the experimental methodology employed to investigate the distribution of trap centers indicated that one of the peaks extended between 0.06 and 0.13 eV, while the other spanned from 0.14 to 0.31 eV. Notably, our research uncovers a remarkable variation in trap density, spanning one order of magnitude, for every 10 and 88 meV of energy variation. The results of our research present the characteristics of shallow trap centers in InSe, providing important information for the design and optimization of InSe-based optoelectronic devices.

Keywords: InSe, 2D materials, defects, TSC, thermoluminescence, optoelectronic devices

Published by OPTICAL MATERIALS
<https://doi.org/10.1016/j.optmat.2024.114959>

1. Introduction

Layered mono-chalcogenides have been the subject of extensive investigation over an extended period due to their broad and alluring spectrum of potential applications [1,2]. Recent research endeavors have been notably centered on exploring the two-dimensional (2D) configurations of the layered compounds. In particular, InSe, a representative member of the layered mono-chalcogenide group, has garnered substantial interest across various application domains [3-6]. 2D structured InSe exhibits a set of noteworthy attributes including ultrahigh electron mobility, modifiable light absorption properties, remarkably high photoresponse, and narrow band gap. These remarkable attributes position InSe as a promising candidate for contemporary nanodevice technologies [7,8]. A recent investigation into 2D InSe revealed its potential utility in flexible electronics and spintronic devices, primarily owing to its low Young's modulus [9]. InSe possesses a direct bandgap of approximately 1.2 eV which provides considerable attention to InSe for solar cell applications. Furthermore, InSe is recognized as a compelling material for constructing heterostructures, with different compounds [10]. InSe exhibits a layered crystalline structure, a salient feature particularly pertinent to the realm of two-dimensional (2D) device technology [11]. The structural arrangement of InSe entails the presence of four covalently bonded Se-In-In-Se atomic planes within each layer, with interlayer interactions primarily governed by van der Waals forces. The distinct crystalline variants of InSe, denoted as ϵ , β , and γ , are attributable to variations in the stacking sequences of these atomic layers. Notably, the β and γ polytypes are of particular interest in InSe-based optoelectronic device technology owing to their propensity for direct band gap characteristics [12-14]. The crystal structure of γ -InSe has been documented as rhombohedral, while that of ϵ - and β -InSe manifests as hexagonal in nature [15].

The identification and characterization of defect centers within semiconductor materials hold remarkable significance for their technological applications. Defects wield the capacity to exert influence over the properties of semiconductors. The discernment of these defect centers empowers researchers to devise strategies aimed at enhancing the device performance constructed from such semiconductors [16]. The revelation of defect centers is an indispensable prerequisite for guiding critical facets of technological applications. Among the methodologies employed for the determination of defect centers, thermally stimulated current (TSC) measurements stand out as a robust and well-established experimental technique for investigating defects within these materials [17]. Defect centers in the InSe compound have previously been revealed in several theoretical and experimental studies. The

characteristics of intrinsic defects in InSe was investigated by density functional theory [18]. It was reported that Se-rich material presents Se_{In} antisite defect where indium interstitial and selenium vacancy are dominant defects in the In-rich material. The analysis of minority carrier transient spectroscopy resulted in presence of hole levels located at 0.12, 0.22 and 0.45 eV [19]. The shallow trap centers were revealed by carrying out space charge limited currents, photoconductivity and TSC experiments [20]. Four trapping centers at 0.06, 0.10, 0.16 and 0.34 eV were from the analyses of the observed spectra. However, no studies on the distribution of trap centers are found in the literature. In the present study, our primary objective is to identify the shallow trap centers within InSe single crystal and reveal traps distribution parameters using the TSC method. The TSC measurements were conducted over a temperature range spanning 10 to 280 K. Subsequent analysis of TSC spectrum facilitated determination of activation energies associated with these trap centers. The distribution parameters of the trap centers were obtained from analysis of TSC data obtained by excitation of the crystal at different temperatures.

2. Experimental details

High-purity elemental materials were used in precise proportions to grow semiconducting polycrystals of InSe. These polycrystals were transformed into layered single crystals using the Bridgman method. This transformation took place within evacuated silica tubes with a diameter of 1 cm and a length of 25 cm, featuring a tip at the bottom. The process involved moving the ampoule through a vertical furnace with a thermal gradient of 30 °C/cm, transitioning from 1000 to 650 °C at a rate of 0.5 mm/h. Atomic compositional ratio of the In and Se in the grown crystal was determined from the energy dispersive spectroscopy analysis in our previous study as In:Se \equiv 49.2:50.8 [21]. The optical image of the InSe single crystal was also represented in this reference. The resulting crystal were dark grey in color and exhibited good optical quality. To analyze the crystalline characteristics, x-ray diffraction (XRD) technique was employed with a Rigaku miniflex XRD system (0.154 nm Cu-K α source). For TSC measurements, a sandwich configuration was utilized for electrical contact. A conductive copper wire with silver paste connected to the front surface, while the back surface was attached to a grounded sample holder. TSC experiments were conducted in a closed-cycle helium gas cryostat (ARS, Model CSW 202), which maintained the sample temperature within the range of 10 to 280 K. A high-power (3 W) blue light-emitting diode (LED) emitting light at a peak energy of 2.6 eV, which is greater than the band gap energy, was used to illuminate the sample. The flux at the sample position was approximately a few

mW/cm². Firstly, temperature was initially lowered to $T_0 = 10$ K, and the front surface of the crystal was exposed to light with energy exceeding the bandgap for a duration of 300 seconds at T_0 . A voltage of $V_1 = 1$ V was applied during illumination, using a Keithley 228 A voltage/current source. After terminating the light source and allowing a brief dark period, the sample temperature was raised to 280 K at a rate of $\beta = 1.0$ K/s. This temperature control was achieved with a Lake-shore temperature controller, maintaining a bias voltage of $V_2 = 100$ V. Keithley 6485 picoammeter was used to record the current. All measurement devices were controlled through a Labview graphical development program, and the TSC measurements were successfully conducted. The schematic diagram of the used system for TSC experiments was reported in Ref. [22].

3. Results and discussions

Figure 1 represents the XRD pattern of InSe crystal. As a result of the measurement taken in the range of 5-80°, five peaks were observed around 10.50, 21.00, 31.95, 42.05 and 63.30°. When the results of the XRD studies of InSe are examined, it is seen that these peaks are related to the hexagonal structure with lattice constants of $a = b = 4.05$ Å nm and $c = 16.93$ Å [23]. When the relevant Miller indices are examined, it is seen that the InSe crystal surface is oriented parallel to (003) plane.

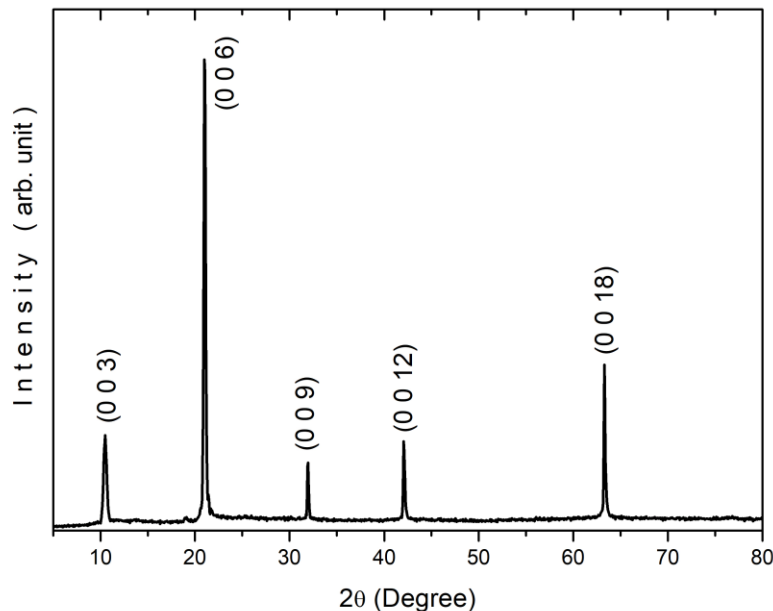


Figure 1. XRD pattern of the InSe single crystal.

TSC measurements were performed on InSe single crystal within a temperature range spanning from 10 to 280 K. The electrical contacts for TSC measurements were fabricated using a sandwich configuration. A copper wire was affixed to the front surface by applying silver paste over the wire, while the other surface was secured to the sample holder with silver paste (See inset of Figure 2). The I-V characteristics of the crystal were examined at room temperature prior to being placed in the cryostat. The I-V behavior demonstrated that the crystal prepared for TSC measurements exhibits ohmic behavior, as illustrated in Figure 2.

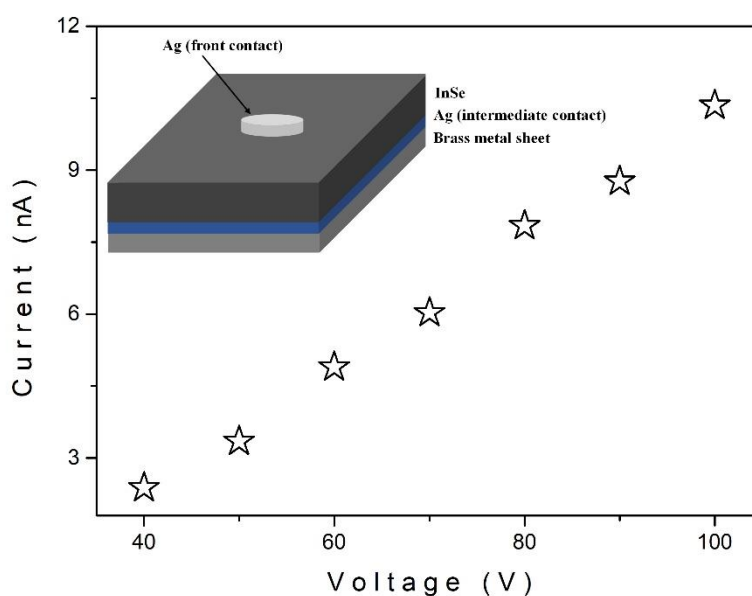


Figure 2. Room temperature I-V plot of the InSe crystal. Inset indicates the sandwich configuration for TSC experiments.

TSC measurements yielded two peaks, each with its maximum temperature point occurring at approximately 82 and 104 K, as visually represented in Figure 3. To ascertain the type of charge carriers involved in the TSC experiments, a selective illumination technique was applied to a single contact on the crystal. Figure 3 illustrates the TSC curves for the InSe crystal under both forward and reverse bias conditions. In this experimental procedure, the contact on the illuminated surface was connected to either the positive or negative terminals of the applied voltage. When the crystal surface was illuminated, it generated both charge carrier types. However, only one type persisted across the entire field, while the opposite one was promptly collected [24]. Figure 3 indicated that when the polarity was positive, the TSC curve showed the higher intensity, pointing out the distribution and subsequent trapping of

holes within the crystal. Hereby, it can be concluded that the observed peaks are characterized as hole traps.

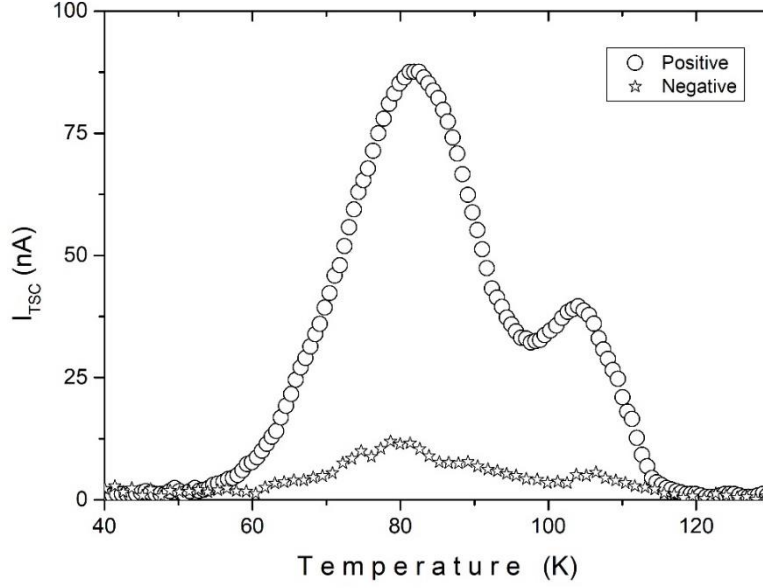


Figure 3. TSC glow curves observed for positive and negative polarities.

The curve fit method was used to obtain the trap activation energies related with the peaks observed in the TSC spectrum. This method is based on the adjustment of the observed TSC curve, taking into account temperature-dependent theoretical equation of current. The temperature-dependent current (I_{TSC}) functions of a single TSC peak are expressed as follows [17]

$$I_{TSC} = C \exp \left\{ -\frac{E_t}{kT} - \int_{T_0}^T \frac{v}{\beta} \exp \left(-\frac{E_t}{kT} \right) dT \right\} \quad (\text{first-order kinetics}) \quad (1)$$

$$I_{TSC} = C \exp \left(-\frac{E_t}{kT} \right) \left[1 + (b-1) \frac{n_0 v}{\beta N} \int_{T_0}^T \exp \left(-E_t/kT \right) dT \right]^{-\frac{b}{b-1}} \quad (\text{non-first order kinetics}) \quad (2)$$

where C : constant, n_0 : initial trapped concentration, N : total trap center concentration, v : attempt-to-escape frequency, and b : order of kinetics parameter taking value $1 < b \leq 2$ for non-first order of kinetics. First and non-first order kinetics correspond to slow and fast retrapping, respectively. The fitting process was successful, especially when dealing with slow retrapping. This suggests that retrapping can be considered negligible for traps within InSe. In Figure 4, the solid line is the fitted curve, and it shows a well-matched pattern with two distinct peaks, each characterized by specific activation energies: $E_{tA} = 0.06$ eV and $E_{tB} = 0.14$

eV. The peak temperatures corresponding to these deconvoluted curves were determined through the fitting process to be $T_A = 81.8$ K and $T_B = 103.9$ K.

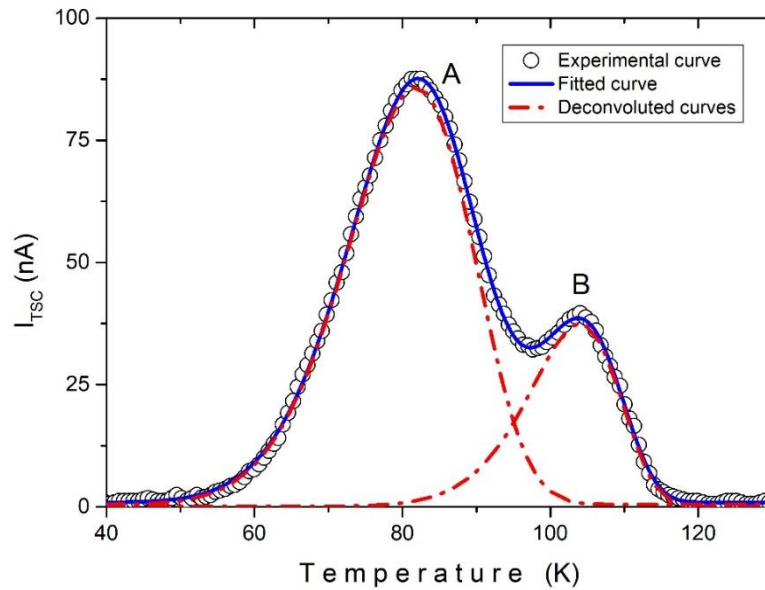


Figure 4. Experimental glow curve and curve fit analysis results.

The trap centers in the bandgap can generally exist as a distribution instead of being a single level. The distribution of traps in the bandgap has potential to affect the electrical behavior of semiconductors. Experts working on semiconductor device design can carry out studies on the characterization of trap centers in order to optimize semiconductor devices such as transistors, diodes, solar cells [25,26]. For this purpose, the following experimental method was used to investigate the distribution of the traps in the InSe crystal [27,28]: The crystal illuminated at $T_{exc.} = 10$ K was heated to certain stopping temperature (T_{stop}), and after the heating was stopped at this temperature, the crystal was cooled back to the first low temperature. TSC curves were obtained by heating the sample from 10 to 280 K without additional illumination. By applying a method in this way, the traps up to the T_{stop} value were emptied. The obtained TSC curve is formed due to the holes coming from the filled traps in the distribution. Figure 5 shows the TSC curves obtained at different T_{stop} values. As the T_{stop} value increases, the TSC curves shift to high temperatures and decrease in intensity indicate the distribution of the trap centers. The TSC curve obtained at $T_{stop} = 85$ K shows that no hole comes from the trap center “A”. Each TSC curve in Figure 5 was analyzed and activation energies of the trap centers were obtained. Figure 6 shows the T_{stop} dependence of the

activation energies obtained as a result of the analyzes. By increasing the T_{stop} value to 73 K, the activation energy of the trap center “A” increased to 0.13 eV. Similarly, increasing the T_{stop} value up to 100 K resulted in an increase in the activation energy of the trap center “B” up to 0.31 eV.

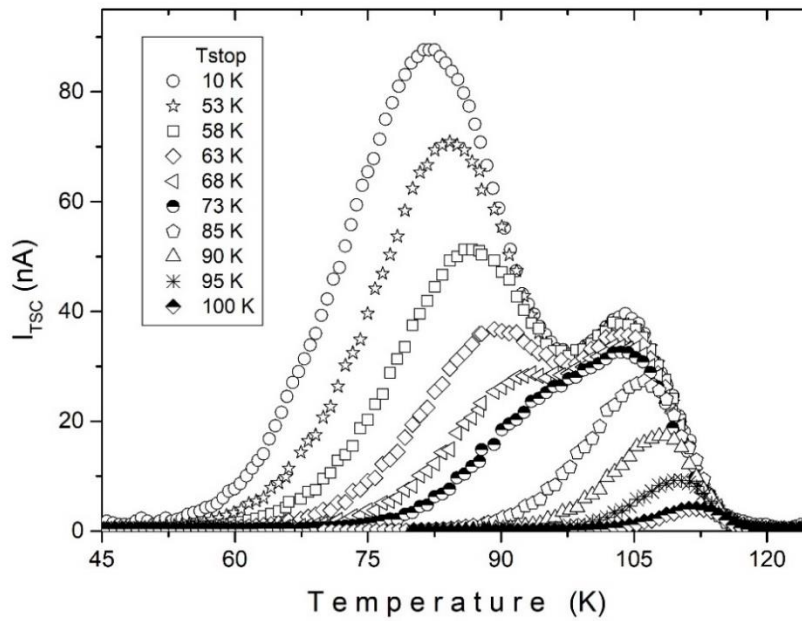


Figure 5. TSC glow curves observed at different stopping temperatures.

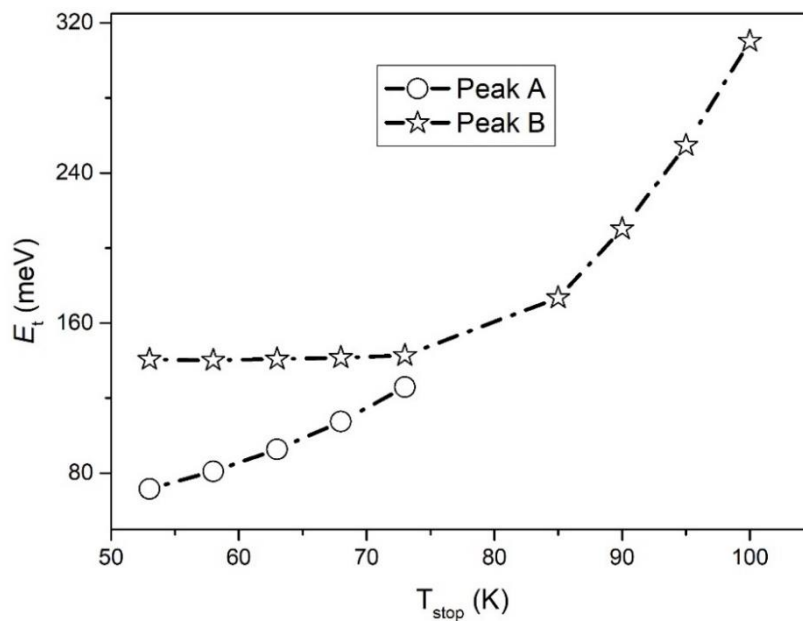


Figure 6. Excitation temperature dependent activation energies of the revealed trapping centers in InSe single crystal.

Given an exponential distribution of traps, with a density of N at energy E_t represented as $N = A_1 \exp(-\alpha E_t)$, we can formulate the following expression occupied at stopping temperature of T_{stop} [29]

$$S_0(I_m/I_e) \propto A_1 \exp(-\alpha E_t). \quad (3)$$

Here, α represents energy parameter characterizing the traps distribution. Furthermore, I_m and I_e denote currents at peak temperature in darkness and during light exposure, respectively. S_0 denotes the area of the TSC peak, directly reflecting the total number of carriers released from the traps as the material is heated. When graphing $\ln[S_0(I_m/I_e)]$ against E_t , a straight line emerges with a slope equal to “ α ”. Figure 7 shows the graph mentioned. The S_0 values used when plotting the graph are the areas under the curves obtained by the curve fit method. As a result of fitting the linearly dependent data in the figure, the energy parameters for peaks were found as $\alpha_A = 0.06034 \text{ meV}^{-1}$ and $\alpha_B = 0.02926 \text{ meV}^{-1}$. These values correspond to 38 and 79 meV/decade, an order of magnitude change in the trap density for every 38 and 79 meV for traps A and B, respectively.

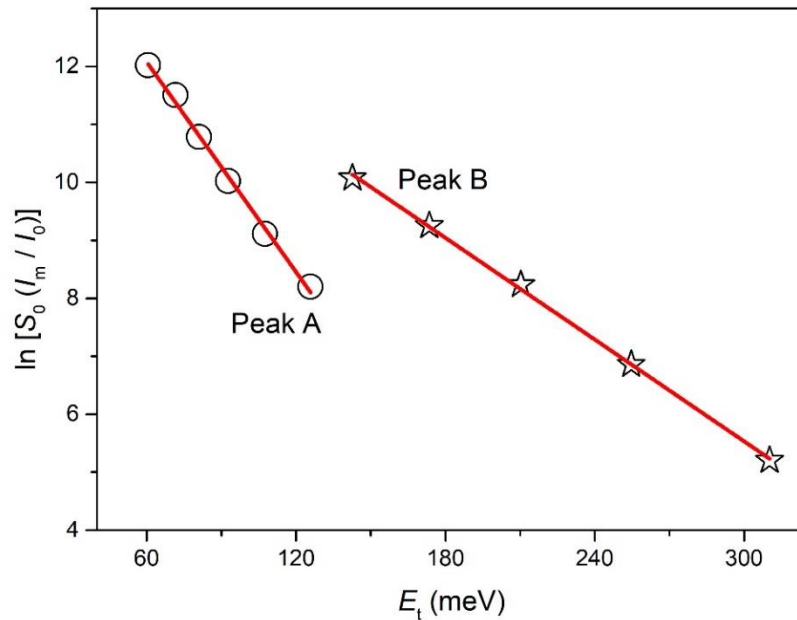


Figure 7. Traps distribution analyses considering the Eq. (3). Solid lines indicate the linear fitted lines.

4. Conclusion

In the present paper, thermally stimulated current method was used to get trap centers in InSe single crystal and investigate distribution of revealed trapping centers. Our comprehensive investigation employing the TSC method has unveiled presence of two trap centers within the InSe crystal. Using the curve fit analysis method, activation energies of trap centers were revealed as 0.06 and 0.14 meV. When the TSC curves obtained from illumination of opposite contacts were compared, it was understood that the trap levels are associated with hole centers. As a result of the experimental method, we applied to examine the distribution of the trap centers, results pointed out that one of the peaks ranged from 0.06 to 0.13 eV and the other from 0.14 to 0.31 eV. The analysis of the experimental data, we observed a change in trap density spanning one order of magnitude for every 38 and 79 meV of variation. The result of the present paper not only contributes to our fundamental understanding of InSe semiconductor behavior but also holds significant promise for advancing the development of novel electronic and optoelectronic devices.

References

- [1] C. Odaci, W. Muehleisen, U. Aydemir, A. Roshanghias, Fabrication and Characterization of Printed Phototransistors Based on Monochalcogenide Inks, *ACS Appl. El. Mater.* 5 (2023) 2007-2016.
- [2] Z.F. Chen, W. Hwang, M. Cho, A.T. Hoang, M. Kim, D. Kim, D.H. Kim, Y.D. Kim, H.J. Kim, J.H. Ahn, A. Soon, H.J. Choi, In-plane optical and electrical anisotropy in low-symmetry layered GeS microribbons, *NPG Asia Mater.* 14 (2022) 41.
- [3] L.J. Luan, L.Y. Han, D. Zhang, K.Y. Bai, K.L. Sun, C.Y. Xu, L. Li, L. Duan, Tuning electronic properties of Z-scheme InSe/HfS₂ heterostructure by external electric field and biaxial strain, *Mater. Sci. Semicon. Proc.* 166 (2023) 107753.
- [4] K. Kumar, M. Sharma, Outstanding intrinsic carrier mobility and transport properties of environmentally stable MX (M=Ga, In; X= S, Se, Te) atomic nanowires, *Physica B* 663 (2023) 414999.
- [5] Z. Wang, Z.H. Wu, X.J. Li, Electronic and optical properties of monolayer InSe quantum dots, *Semicond. Sci. Tech.* 36 (2021) 095038.
- [6] Z. Chang, K.P. Yuan, Z.H. Sun, X.L. Zhang, Y.F. Gao, G.Z. Qin, D.W. Tang, Ultralow lattice thermal conductivity and dramatically enhanced thermoelectric properties of monolayer InSe induced by an external electric field, *Phys. Chem. Chem. Phys.* 23 (2021) 13633-13646.
- [7] H. Wang, G.Y. Xian, L. Liu, X.Y. Liu, H. Guo, L.H. Bao, H.T. Yang, H.J. Gao, InSe-Te van derWaals heterostructures for current rectification and photodetection, *Chinese Phys. B* 32 (2023) 087303.

- [8] Q.H. Zhao, P. Chen, D. Zheng, T. Wang, A. Castellanos-Gomez, R. Frisenda, Multifunctional indium selenide devices based on van der Waals contacts: High-quality Schottky diodes and optoelectronic memories, *Nano Energy* 108 (2023) 108238.
- [9] Q.H. Zhao, R. Frisenda, T. Wang, A. Castellanos-Gomez, InSe: a two-dimensional semiconductor with superior flexibility, *Nanoscale* 11 (2019) 9845.
- [10] Y. Cen, Y. Tu, J. Zhu, Y. Hu, Q. Hao, W. Zhang, Photoinduced Contact Evolution and Junction Rearrangement in Two-Dimensional van der Waals Heterostructure, *Adv. Funct. Mater.* 33 (2023) 2306668.
- [11] M.J. Dai, C.F. Gao, Q.F. Nie, Q.J. Wang, Y.F. Lin, J.H. Chu, W.W. Li, Properties, Synthesis, and Device Applications of 2D Layered InSe, *Adv. Mater. Technol.* 7 (2022) 2200321.
- [12] B. Zhang, H. Wu, K. Peng, X. Shen, X. Gong, S. Zheng, X. Lu, G. Wang, X. Zhou, Super deformability and thermoelectricity of bulk γ -InSe single crystals, *Chinese Phys. B* 30 (2021) 078101.
- [13] K. Yuxuan, L. Chun, X. Zhang, J. Song, R. Li, L. Liu, J. Dai, Z. Wei, Q. Zhang, Giant enhancement of second-harmonic generation of indium selenide on planar Au, *Nanoscale* 15 (2023) 10125-10132.
- [14] Z.N. Guo, R. Cao, H.D. Wang, X. Zhang, F.X. Meng, X. Chen, S.Y. Gao, D.K. Sang, T.H. Nguyen, A.T. Duong, J.L. Zhao, Y.J. Zeng, S. Cho, B. Zhao, P.H. Tan, H. Zhang, D.Y. Fan, High-performance polarization-sensitive photodetectors on two-dimensional β -InSe, *Natl. Sci. Rev.* 9 (2022) nwab098.
- [15] L. Debbichi, O. Eriksson, S. Lebegue, Two-Dimensional Indium Selenides Compounds: An Ab Initio Study, *J. Phys. Chem. Lett.* 6 (2015) 3098-3103.
- [16] L.P. Liao, E. Kovalska, J. Luxa, L. Dekanovsky, V. Mazanek, L. Valdman, B. Wu, S. Huber, M. Mikulics, Z. Sofer, Unraveling the Mechanism of the Persistent Photoconductivity in InSe and its Doped Counterparts, *Adv. Opt. Mater.* 10 (2022) 2200522.
- [17] R. Chen, Y. Kirsh, *Analysis of Thermally Stimulated Processes*, Pergamon Press, Oxford, 1981.
- [18] K.J. Xiao, A. Carvalho, A.H. Castro Neto, Defects and oxidation resilience in InSe, *Phys. Rev. B* 96 (2017) 054112.
- [19] G. Micocci, P. Siciliano, A. Tepore, Hole traps in n-InSe single crystals by minority-carrier transient spectroscopy measurements, *Sol. Energ. Mater.* 20 (1990) 131-138.
- [20] M. Di Giulio, G. Micocci, L. Ruggiero, A. Tepore, F. Zuanni, Trapping centers in InSe single crystals, *Mater. Chem. Phys.* 9 (1983) 329-339.
- [21] M. Isik, N.M. Gasanly, Temperature-tuned band gap characteristics of InSe layered semiconductor single crystals, *Mater. Sci. Semicond. Process.* 107 (2020) 104862.
- [22] M. Isik, S. Delice, N.M. Gasanly, Investigation of defect levels in Bi₁₂SiO₂₀ single crystals by thermally stimulated current measurements, *Phys. Scr.* 96 (2021) 125875.
- [23] D.K. Sang, H. Wang, M. Qiu, R. Cao, Z. Guo, J. Zhao, Y. Li, Q. Xiao, D. Fan, H. Zhang, Two Dimensional β -InSe with Layer-Dependent Properties: Band Alignment, Work Function and Optical Properties, *Nanomaterials* 9 (2019) 82.
- [24] M. Isik, S. Delice, N.M. Gasanly, N.H. Darvishov, V.E. Bagiev, Trapping centers in Bi₁₂TiO₂₀ single crystals by thermally stimulated current, *Opt. Mater.* 122 (2021) 111797.

- [25] Y.Y. Yan, V. Kilchytska, D. Flandre, J.P. Raskin, Investigation and optimization of traps properties in Al₂O₃/SiO₂ dielectric stacks using conductance method, *Solid State Electron.* 194 (2022) 108347.
- [26] F. Winterer, L.S. Walter, J. Lenz, S. Seebauer, Y. Tong, L. Polavarapu, R.T. Weitz, Charge Traps in All-Inorganic CsPbBr₃ Perovskite Nanowire Field-Effect Phototransistors, *Adv. Electron. Mater.* 7 (2021) 2100105.
- [27] S.N. Singh, Analysis of the thermoluminescent of borate glass by computerized glow curve deconvolution in kinetic formalism, *J. Phys. Conf. Ser.* 2070 (2021) 012009.
- [28] M. Molano-Mendoza, R. Melendrez, L.A. Gonzalez, Thermoluminescence of beta irradiated SrHfO₃ powders synthesized by the Pechini-type sol-gel method, *J. Lumin.* 263 (2023) 120048.
- [29] M. Isik, N.M. Gasanly, Trapping centers and their distribution in Tl₂Ga₂Se₃S layered single crystals, *J. Phys. Chem. Sol.* 70 (2009) 1048-1053.